

# Processing of a porous titanium alloy from elemental powders using a solid state isothermal foaming technique

Aris W. Nugroho · Garry Leadbeater · Ian J. Davies

Received: 17 March 2010 / Accepted: 21 September 2010 / Published online: 20 October 2010  
© Springer Science+Business Media, LLC 2010

**Abstract** The authors have conducted a preliminary investigation with regard to the potential to manufacture porous titanium alloys for biomedical applications using toxic-free elemental powders, i.e., Ti, Nb, Ta, Zr, in combination with the pressurised gas bubble entrapment method and in contrast to standard processing routes that generally utilise prealloyed powder containing potentially toxic elements. Elemental powder compacts were either hot isostatic pressed (HIP-ed) at 1000°C and then foamed at 1150°C or else HIP-ed at 1100°C and foamed at 1350°C. Porous  $\alpha + \beta$  alloys containing up to 45 vol% of porosity in the size range 20–200  $\mu\text{m}$  were successfully produced, thus highlighting the potential of this manufacturing route. It was expected that further optimisation of the processing route would allow full development of the preferred  $\beta$ -Ti phase (from the point of view of elastic modulus compatibility between implant and bone) with this being the subject of future work by the authors.

## 1 Introduction

Whilst titanium (Ti) and its alloys are widely used for biomedical applications such as bone repair or reconstruction due to their excellent biocompatibility, high specific strength and high corrosion resistance [1], a number of issues concerning the use of these materials still

exist. For example, the difference in Young's modulus between implanted materials such as commercial purity (CP) Ti (105 GPa) or Ti–6Al–4V (110 GPa) and compact bone (10–40 GPa) [2] is known to result in stress shielding effects, although this can be overcome through the use of porous Ti alloys. Secondly, health issues concerning alloying elements commonly used in the production of  $\alpha$ -phase Ti alloys have also been raised; nickel and chromium are known to be metal allergens [3] whereas the use of vanadium and aluminium has been linked to cytotoxic tissue reactions and potential neurological disorders, respectively [4]. In light of this, the use of non-toxic  $\beta$ -stabilising elements such as Nb, Ta and Zr has been reported to result in alloys with good biocompatibility [5] with these elements also being expected to result in alloys with enhanced strength and decreased elastic modulus [6]—the use of  $\beta$ -phase Ti being preferred to that of  $\alpha$ -phase due to its significantly lower elastic modulus (102–105 GPa compared to 55–85 GPa [7]).

Another potential issue is that titanium alloys are categorised as bioinert materials such that the attachment of Ti based materials into bone may lead to encapsulation by dense fibrous tissues resulting in a weak bone implant interface, loosening of the implant and fixation failure [8]. However, the introduction of porosity into the implant material, in addition to improving the compatibility in stiffness between implant and bone, may also promote the entrapment of specific proteins such as vitronectin and fibronectin and thus enhance osteoblastic cell attachment, proliferation and differentiation on the implant surface [9, 10]. Additional bone development within the pores and bonding with adjacent tissue can also provide mechanical interlocking between the bone and implant material. Therefore, the use of porous Ti alloys employing non-toxic elements has the potential to increase fixation of the

---

A. W. Nugroho · G. Leadbeater (✉) · I. J. Davies  
Department of Mechanical Engineering, Curtin University  
of Technology, GPO Box U1987, Perth, WA 6845, Australia  
e-mail: G.Leadbeater@curtin.edu.au

A. W. Nugroho  
Department of Mechanical Engineering, Muhammadiyah  
University of Yogyakarta, Yogyakarta 55183, Indonesia

implant whilst reducing stress shielding effects and therefore prolong device life-times.

Several solid state processing routes have been developed to produce porous Ti alloys for use in orthopaedic applications. Whilst the sintering of compacted loose powder normally results in low porosities [2], the space holder technique (in which spacer particles such as ammonium hydrogen carbonate, magnesium, or polymeric materials [11] are utilised) has resulted in the manufacture of pure titanium foam with high porosity levels (70–80%); however, contamination of the Ti during removal of the spacer remains a significant concern. The use of inert gases such as argon have also been applied to promote porosity due to the expansion of pressurised argon bubbles within the metal matrix at elevated temperature [12] with the amount and morphology of the porosity being related to parameters such as the back fill pressure, foaming temperature and holding time [13, 14]. Whilst this latter technique has led to the development of porous pure titanium and titanium alloys based on prealloyed starting powder [12, 15], the starting (i.e., prealloyed) powder generally contains lower levels of biocompatible elements and is expensive when compared to the use of elemental powders.

Therefore, the authors have investigated the use of pressurised bubble entrapment in the manufacture of porous (preferably  $\beta$ -phase) titanium alloys based on non-toxic elemental starting powders (Ti, Ta, Nb, Zr) with initial results being presented in this work—a key aspect of this research being that elemental starting powders were used instead of traditional prealloyed powder.

## 2 Materials and methods

The starting elemental powders utilised in this work, namely Ti (99.5% purity), Nb (99.9%), Ta (99.7%), and Zr (99.5%) (CERAC Inc., Milwaukee, USA) possessed a wide particle size distribution below 44  $\mu\text{m}$  with an angular particle morphology (Fig. 1a). The elemental powders were weighed to give a nominal composition of Ti–29Nb–13Ta–4.5Zr and then blended for 30 min in a roller mixer. Following this, approximately 50 g of alloy powder was placed into a stainless steel can with an inner diameter and length of 28 and 30 mm, respectively. Each can was subsequently evacuated to approximately  $10^{-2}$  Pa and then backfilled with 0.48 MPa of argon and sealed. The pressurised cans were then densified using hot isostatic pressing (HIP) at 1000°C for 2 h or 1100°C for 4 h under 100 MPa of argon (Australian Nuclear Science and Technology Organisation, Sydney, Australia) and then furnace cooled. Cubic specimens of approximate dimension 10 mm were cut from the centre of each HIP-ed billet using electro

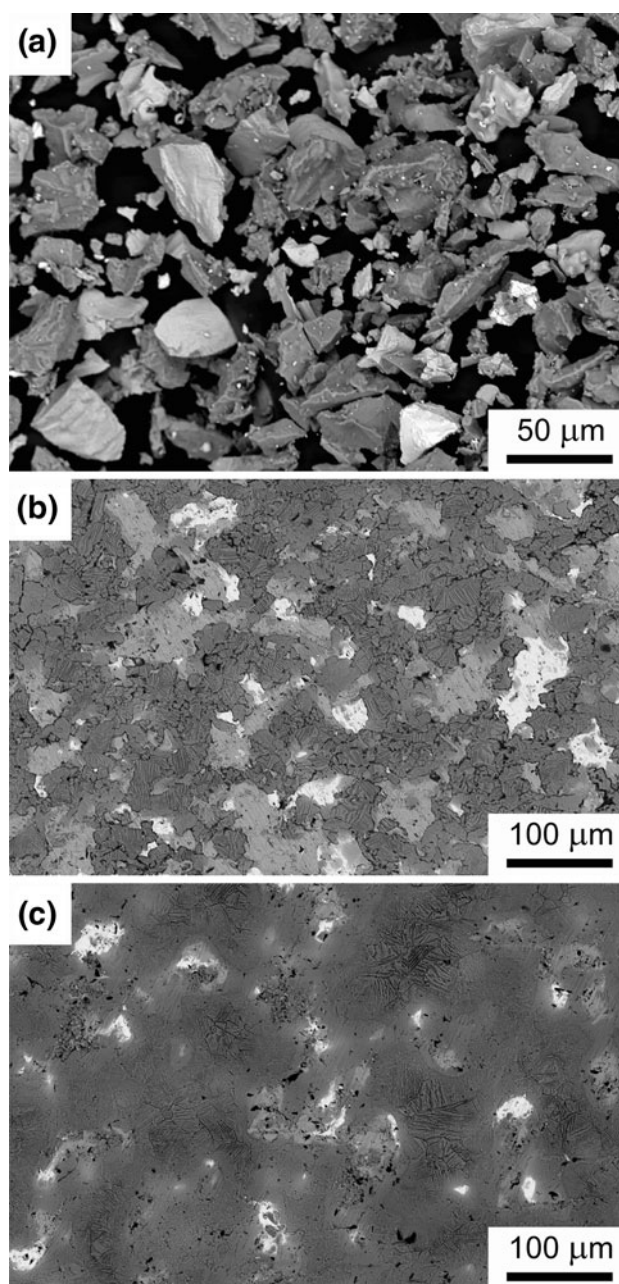


**Fig. 1** Backscattered scanning electron micrographs: **a** illustrating the size and morphology of the blended powder, and illustrating the grain structure and degree of reaction for the Ti–Nb–Ta–Zr specimens following HIP-ing in argon: **b** 1000°C/2 h/100 MPa, and **c** 1100°C/4 h/100 MPa

discharge machining (EDM) and followed by light polishing with 600 grit silicon carbide paper and ultrasonic cleaning using acetone in order to remove the EDM-damaged surface layer.

The HIP-ed billet specimens were then rapidly heated in a graphite element vacuum furnace to 1150°C (for the 1000°C HIP-ed specimens) or 1350°C (for the 1100°C HIP-ed specimens) and held for 10 h (isothermal foaming process)—the two processing conditions employed in this

work were considered to represent the lower and upper bounds of processing conditions in order to produce  $\beta$ -Ti. During this time the pressurised pores were expected to expand due to creep of the surrounding metal. Previous researchers had found that pore sizes grew rapidly during the initial 10 h of foaming [12] with no further growth being noted after approximately 3 days of foaming [16].

Following this foaming process, selected specimens were metallographically prepared by grinding and polishing to 0.05  $\mu\text{m}$ . The amount and morphology of any porosity was examined using optical microscopy (OM) and scanning electron microscopy (SEM) following etching using modified Kroll's solution (2.5% HF, 5% HNO<sub>3</sub> and 92.5% H<sub>2</sub>O)—the resulting micrographs were examined using freely available software (ImageJ, National Institutes of Health, USA).

Flat plates of approximate thickness 2 mm for each specimen were investigated using synchrotron radiation diffraction (SRD) on the Powder Diffraction beamline at the Australian Synchrotron facility in Melbourne, Australia. Prior to analysis, each sample was placed onto an aluminium specimen holder that was rotated during the experiment. The synchrotron beam had been passed through a bent Si crystal monochromator with a beam energy of 15 keV (equivalent to a wavelength of 0.08263 nm). The beam width and height were 2.0 and 0.2 mm, respectively, whilst the beam angle incident to the specimen was kept constant at 5°. In order to allow easier comparison with standard X-ray diffraction (XRD) data, the SRD results for each specimen were converted into angular data equivalent to the wavelength of Cu K $\alpha$  (i.e., 0.15418 nm).

### 3 Results and discussion

Typical synchrotron radiation diffraction patterns for specimens before and after HIP-ing have been presented in Fig. 2. As expected, peak identification for the blended powder pattern (Fig. 2a) indicated the presence of peaks related to the individual elements; the structure of Ti and Zr was hexagonal close packed (hcp) whereas that of Nb and Ta was isomorphous body centered cubic (bcc). Following HIP-ing the SRD patterns of the specimens HIP-ed at 1000°C (Fig. 2b) and 1100°C (Fig. 2c) were both found to contain peaks attributed to  $\alpha$ - and  $\beta$ -Ti, Nb and Ta with an absence of peaks related to elemental or intermetallic Zr (as had been noted by previous researchers [17]). This result was consistent with the fact that peaks related to  $\alpha$ -Ti are known to be suppressed as the HIP-ing temperature is increased above 1000°C (due to the conversion of  $\alpha \rightarrow \beta$ ) with the transformation being complete beyond 1500°C [17]. It was thus concluded that the HIP-ing procedure had

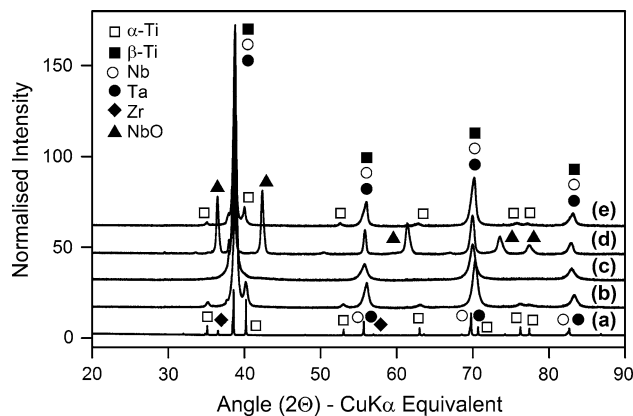


**Fig. 2** Synchrotron radiation diffraction (SRD) plots of the Ti–Nb–Ta–Zr specimens: (a) mixed elemental powder, (b) after densification by hot isostatic pressing in argon (1000°C/2 h/100 MPa), (c) after densification by hot isostatic pressing in argon (1100°C/4 h/100 MPa), (d) after isothermal foaming at 1150°C/10 h, (e) after isothermal foaming at 1350°C/10 h. Note that the presence of NbO in the specimen foamed at 1150°C was attributed to reduced vacuum conditions during a portion of the treatment

resulted in the partial conversion of  $\alpha$ -phase to  $\beta$ -phase within the alloys with the aim being to complete the conversion process during the subsequent foaming operation.

A typical backscattered SEM micrograph of the specimen HIP-ed at 1000°C indicated the presence of angular titanium particles (dark), niobium (grey) and tantalum (bright), i.e., similar to the initial particle morphology (Fig. 1b). In contrast to this, the specimen HIP-ed at 1100°C indicated the particle boundaries to have become diffuse (Fig. 1c) due to the partial dissolution of Nb and Ta particles within the HIP-ed specimens. Although not shown here, the combination of HIP-ing (1100°C) above the  $\alpha \rightarrow \beta$  transformation temperature (1000°C) and subsequent slow cooling to room temperature under vacuum was believed to have resulted in the beginning of a two phase ( $\alpha + \beta$ ) Widmanstätten structure that developed due to the dissolution of Nb particles; this was particularly apparent for the case of titanium particles in regions of the specimen where dissolution of the  $\beta$ -stabiliser elements had taken place more slowly. The Ti–Nb–Ta–Zr alloys following HIP-ing were thus classified as being  $\alpha + \beta$  with the Widmanstätten structure in the 1000°C specimen potentially acting as a  $\beta$ -phase nucleator agent during higher HIP-ing and/or foaming temperatures [17].

The HIP-ed specimens (1000 and 1100°C) were found to contain pores that were attributed to incomplete dissolution between the elemental powders with the pore sizes (typically 10  $\mu\text{m}$ ) being similar to that of the original inter powder spacing. The total porosity in the HIP-ed specimens was estimated to be <3 vol% (1000°C) and <1 vol% (1100°C) which is consistent with previous researchers

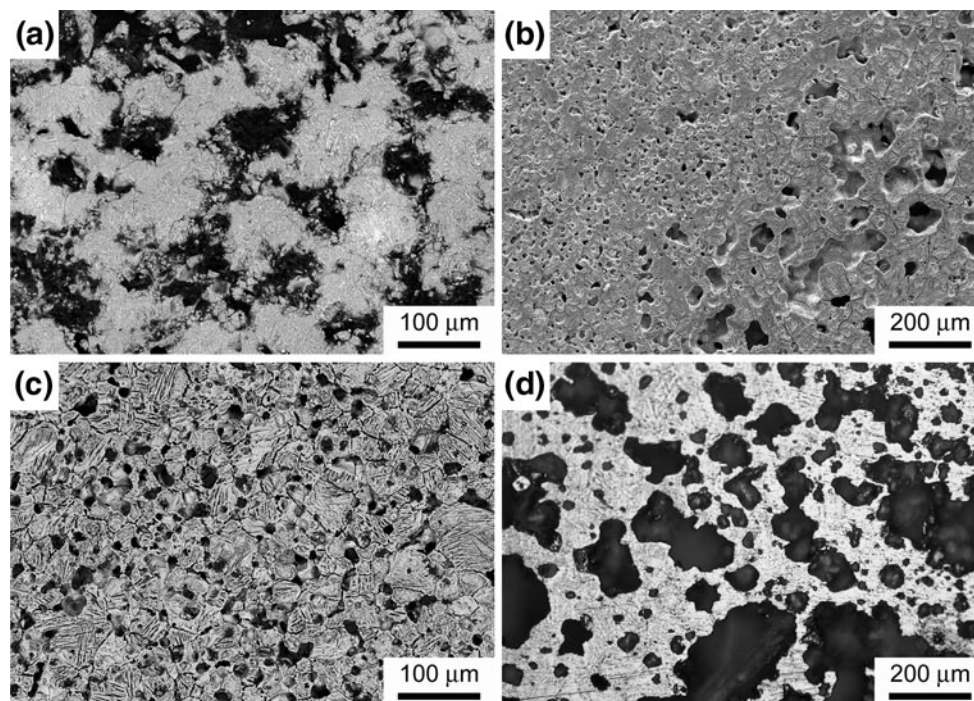


**Fig. 3** Scanning electron and optical micrographs of the Ti-Nb-Ta-Zr specimens foamed in argon: **a** 1150°C/10 h (SEM), **b** 1350°C/10 h (SEM), **c** centre (SEM), and **d** edge of the 1350°C/10 h specimen (OM)

who noted initial porosity levels between approximately 0.14–2.4 vol% for HIP-ed CP-Ti [16].

Backscattered SEM and OM micrographs illustrating pore morphologies for the specimens foamed at 1150 and 1350°C using a backfilled argon pressure of 0.48 MPa have been presented in Fig. 3. The specimen foamed at 1150°C was noted to contain approximately 30 vol% porosity (Fig. 3a) with the pore size and morphology being reasonably uniform across the specimen. On the other hand, the pore size distribution in the specimen foamed at 1350°C was varied (Fig. 3b) with the pores at the specimen centre being discrete (i.e., no coalescence) (Fig. 3c) and mainly equiaxed with typical diameters of 20–50  $\mu\text{m}$ ; the porosity in this region was found to be approximately 14 vol%. In contrast to this, close to the specimen surface the pores had noticeably expanded with the porosity level achieving approximately 45 vol% and pore sizes of typically 100–200  $\mu\text{m}$  (Fig. 3d). This phenomenon was attributed to fewer constraints against expansion being present at the surface region of the specimen. Interconnected pores were also found close to the surface suggesting that many pores had coalesced (and thus inter-pore walls had collapsed) due to gas expansion. However, this expansion would presumably be inhibited as the pore volume increased and/or the pressurised argon escaped to the atmosphere as the pores connected to the specimen surface. Overall, the relatively large porosities contained in

the foamed specimens would be expected to result in elastic moduli more compatible with that of bone when compared to standard dense Ti implants.

Pore morphology such as size and interconnectivity are known to be important factors for protein absorption which initiates bone ingrowth into porous implant. Previous research has noted that bone ingrowth into porous coating occurs for pore sizes down to 50  $\mu\text{m}$  [18], while the porosity interconnections should be larger than 100  $\mu\text{m}$  for the generation of mineralised bone [19]. Hence, the porous titanium alloys prepared in this preliminary work may have a pore size diameter appropriate for biomedical implant applications.

Homogenisation of the HIP-ed alloy foamed at 1150°C was found to be still incomplete, indicating that dissolution of Nb and Ta may have continued for additional foaming time. In contrast to this, Ta particles were found to have dissolved following foaming at 1350°C which resulted in a more homogenous microstructure comprising of  $\alpha$  plates and hcp-martensite,  $\alpha'$ , dispersed within a  $\beta$  phase (Fig. 4). The existence of the martensitic phase indicated that the alloy was likely to be an  $\alpha + \beta$  structure. Therefore, the present work has highlighted the possibility of manufacturing porous  $\alpha + \beta$ -Ti from non-toxic elemental powder with the potential existing for complete transformation to  $\beta$ -Ti upon further optimising the processing route.

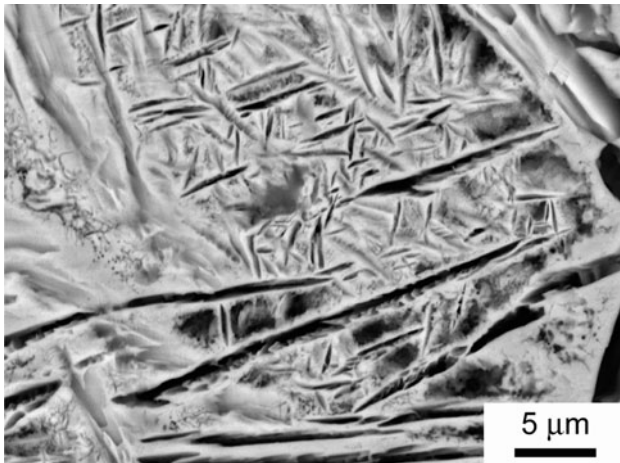


**Fig. 4** Scanning electron micrograph illustrating the martensitic structure of the Ti–Nb–Ta–Zr specimen foamed at 1350°C for 10 h

#### 4 Conclusions

The current study has successfully demonstrated the potential fabrication of porous titanium alloys containing non-toxic elements, i.e., Ti, Nb, Ta, Zr, from elemental powders using a powder metallurgy route and pressurised gas entrapment. The resulting Ti–Nb–Ta–Zr alloys were found to contain porosity amounts and sizes ranging between approximately 20–40 vol% and 20–200 μm, respectively, with some interconnected pores being formed. The porous titanium alloys under investigation are expected to exhibit great potential as a biocompatible implant material due to their porous structure providing a more compatible elastic modulus and allowing the ingrowth of new bone tissue. In future work the authors plan to investigate in detail the influence of processing parameters on the physical characteristics and mechanical behaviour in compression of these alloys.

**Acknowledgments** This study was supported financially by TPSDP, SPMU: Muhammadiyah University of Yogyakarta. The authors also wish to thank the Australian Nuclear Science and Technology Organisation (ANSTO) for carrying out the HIP-ing and foaming procedures. A part of this research was undertaken on the Powder Diffraction beamline at the Australian Synchrotron, Victoria, Australia.

#### References

1. Niinomi M. Recent metallic materials for biomedical applications. *Metall Mater Trans A*. 2002;33:477–86.
2. Oh IH, Nomura N, Masahashi N, Hanada S. Mechanical properties of porous titanium compacts prepared by powder sintering. *Scripta Mater*. 2003;49:1197–202.
3. Hildebrand HF, Veron C, Martin P. Nickel, chromium, cobalt alloys and allergic reactions: an overview. *Biomaterials*. 1989;10: 545–8.
4. Wapner KL. Implications of metallic corrosion in total knee arthroplasty. *Clin Orthop Relat Res*. 1991;271:12–20.
5. Eisenbarth E, Velten D, Muller M, Thull R, Breme J. Biocompatibility of  $\beta$ -stabilizing elements of titanium alloys. *Biomaterials*. 2004;25:5705–13.
6. Song Y, Xu D, Yang R, Li D, Wu WT, Guo ZX. Theoretical study of the effects of alloying elements on the strength and modulus of  $\beta$ -type bio-titanium alloys. *Mater Sci Eng A*. 1999; 260:269–74.
7. Niinomi M. Mechanical properties of biomedical titanium alloys. *Mater Sci Eng A*. 1998;243:231–6.
8. Stojanovic D, Jokic B, Veljovic D, Petrovic R, Uskokovic PS, Janackovic D. Bioactive glass-apatite composite coating for titanium implant synthesized by electrophoretic deposition. *J Eur Ceram Soc*. 2007;27:1595–9.
9. Wilson J, Clegg RE, Leavesley DI, Percy MJ. Mediation of biomaterial-cell interactions by adsorbed proteins: a review. *Tissue Eng*. 2005;11:1–18.
10. Karageorgiou V, Kaplan D. Porosity of 3D biomaterial scaffolds and osteogenesis. *Biomaterials*. 2005;26(27):5474–91.
11. Jee CSY, Özgüven N, Guo ZX, Evans JRG. Preparation of high porosity metal foams. *Metall Mater Trans B*. 2000;31:1345–52.
12. Kearns MW, Blenkinsop PA, Barber AC, Farthing TW. Manufacture of a novel porous metal. *Met Mater*. 1987;3:85–8.
13. Davis NG, Teisen J, Schuh C, Dunand DC. Solid-state foaming of titanium by superplastic expansion of argon-filled pores. *J Mater Res*. 2001;16:1508–19.
14. Ashworth MA, Jacobs MH, Unwin P, Blunn G. In: 7th World Biomaterials Congress-2004, Sydney; 2004.
15. Oppenheimer S. Processing and Characterization of Porous Ti–6Al–4V and NiTi. PhD Thesis, Northwestern University, IL; 2007.
16. Davis NG. Enhancement of solid state foaming of titanium by transformation superplasticity. PhD Thesis, Northwestern University, IL; 2002.
17. Taddei EB, Henriques VAR, Silva CRM, Cairo CAA. Production of new titanium alloy for orthopedic implants. *Mater Sci Eng C*. 2004;24:683–7.
18. Bobyn JD, Cameron H, Weatherly G. The optimum pore size for the fixation of porous-surfaced metal implants by the ingrowth of bone. *Clin Orthop*. 1980;150:263–70.
19. Hulbert S, Young F, Mathews R, Klawiter J, Takbert C, Stelling F. Potential of ceramic materials as permanently implantable skeletal prostheses. *J Biomed Mater Res*. 1970;4:433–56.